Dispatchability Limits for PV Generation in Unbalanced Distribution Networks with EVs

Mohammad Ramin Feizi
Department of Electrical and Computer Engineering
Southern Methodist University
Dallas, Texas, United States
mfeizi@smu.edu

Mohammad E. Khodayar

Department of Electrical and Computer Engineering
Southern Methodist University
Dallas, Texas, United States
mkhodayar@smu.edu

Abstract— The increase in the installed capacity of small-scale photovoltaic generation and the growing demand for electric vehicles introduce operational challenges for the unbalanced distribution networks. This paper presents a two-stage optimization problem to determine the dispatchability limits of photovoltaic generation considering the electric vehicles' interconnection to ensure the security of the distribution network. The uncertainty associated with a) the state of charge at arrival and departure times; b) the energy and power capacity of electric vehicles; c) the maximum forecasted solar radiation and demand were considered. The proposed optimization problem is solved using the column-and-constraint-generation approach. A modified IEEE 13-bus test system is used to evaluate the effectiveness of the proposed framework.

Index Terms-- dispatchability limits, electrical vehicles, photovoltaic generation, unbalanced distribution operation, uncertainty.

I. INTRODUCTION

Electric vehicle (EV) is a promising solution to reduce the carbon footprint and to improve the economics of transportation networks. The increase in the penetration level of EVs introduces challenges to supply energy in the distribution networks including the increase in the real power loss, degradation of assets' lifetime, and reduction in the voltage stability margin of the distribution network [1]-[3]. Distributed renewable energy resources (DERs) are considered as a solution to address some of these challenges. As local generation resources close to the demand, DERs contribute to the reduction in real power loss, and improvement in the voltage profile. Among these resources, solar photovoltaic (PV) generation is the prominent energy resource connected to the distribution networks. The variability and uncertainty in PV generation profile impose technical challenges including voltage rise, reverse power flow and protection malfunction [4]. Curtailing PV generation and coordinating PV generation with energy storage facilities (e.g. battery energy storage or EVs) could mitigate the adverse effects of this technology and

improve the penetration level of solar PV in the distribution networks.

Earlier research addressed the uncertainty in renewable DERs and EVs in the distribution network operation [5]-[8]. A two-level optimization problem is formulated in [5] to maximize the profit of EV parking lot operators and assess the impact of uncertainty of wind and PV generation on the payoff of EV parking lot operators. A two-stage robust optimization problem is formulated in [6] that leverages the conic relaxation of the distribution branch flow to determine the dispatch of PV generation considering the uncertainties in PV output in the distribution networks. A two-stage robust optimization model is proposed in [7] to regulate the real and reactive power in certain distribution branches, to mitigate the voltage violations and to reduce the network loss.

The dispatchability limits for renewable energy resources were addressed in earlier research works [8]-[9]. In [8], the maximum dispatchability limits for wind generation in bulk power network is addressed by formulating a robust optimization problem solved using three approaches. In [9] a data-driven approach is proposed to maximize the utilization of variable wind generation resources by leveraging their dispatchability limits. While such research works addressed the dispatchability limits of renewable energy resources, limited studies were performed on the dispatchability limits of renewable energy resources in the unbalanced distribution networks. The contributions of this paper are as follows:

- Determining the upper and lower bounds for PV generation in the unbalanced distribution network
- Capturing the uncertainty associated with a) the EV interconnection including the state of charge at arrival and departure times as well as the maximum energy and power capacity of EVs connected to the distribution network; b) maximum PV generation and; c) electricity demand in the distribution networks
- The proposed formulated problem is solved using the column-and-constraint-generation (C&CG) approach to determine the worst-case realization of PV

generation considering the determined upper and lower bounds.

The rest of the paper is organized as follows; the problem formulation and solution methodology are presented in Section II. The numerical analysis and conclusion are presented in Sections III and IV respectively.

PROBLEM FORMULATION AND SOLUTION METHODOLOGY

A. Problem formulation

The problem formulation is shown in (1)-(33). The objective function is shown in (1). Here, $u_{v,t}^{\varphi}$ and $l_{v,t}^{\varphi}$ are the upper and lower bounds of PV generation respectively; and $V_{v,t}^{\varphi}$ is the auxiliary binary variable. The objective is to maximize the difference between the lower and upper bounds of PV generation while minimizing the violation in nodal real and reactive power represented by positive slack variables $s_{b,t}^{(.),\varphi}$. The constraints are shown in (2)-(33). The real and reactive power balance at each bus is shown in (2) and (3) respectively. Here, the variables are $PL_{l,t}^{\varphi}$ (the real power of the distribution line l on phase φ at time t), $P_{i,t}^{\varphi}$ (the real power of DG i), $P_{n,t}^{\varphi}$ (the real power of distribution feeder n), $P_{v,t}^{\varphi}$ (the real power of PV v), and $P_{e,t}^{\varphi}$ (the real power of EV cluster e). $P_{d,t}^{\varphi}$ is a parameter which the real power demand. The matrices AL, AI, AV, AE, AN, and AD are the line-bus, distributed generationbus, PV generation-bus, EV cluster-bus, distribution feederbus, and demand-bus incidence matrices respectively. A similar constraint for reactive power $Q_{(.)}^{(.)}$ is shown in (3). The apparent power flow $SL_{l,t}$ satisfies (4) and (5) in which, $U_{k,t}$ is the vector of squared voltage on phases a, b and c of bus k $(V_{k,t}^{(.)})$ as shown in (38); p_l^{φ} is the availability of phase φ of the line $l; \mathbf{Z}_l$ is the element-wise product of matrix \mathbf{A} and the branch impedance matrix \mathbf{z}_l shown in (34)-(36) [10]. Here, \mathbf{r}_l is the resistance and x_i is the inductive reactance matrix of branch l. The vector of apparent power $SL_{l,t}$ is shown in (37). The real and reactive power flows of branch l satisfy (6)-(9) where $SL_l^{\varphi,max}$ is the maximum complex power transmitted through the branch [11]. Similar constraints could be written for the distribution feeder. The real and reactive powers of DG are limited by the minimum and maximum limits as shown in (10) and (11) respectively. The real and reactive powers of feeder satisfy (12) and (13) to maintain the power factor more than a certain value (PF_n) . The real and reactive powers of PV generation are within the limits as shown in (14) and (15). Here, $P_n^{\varphi,max}$ is the maximum nominal capacity of the PV generation. The real power dispatch of PV generation is limited by the available solar radiation as shown in (16). Here, A_{ν}^{φ} is the area of PV generation unit for phase φ and $IR_{\nu,t}$ is solar radiation. The lower and upper bounds for PV generation satisfy (17)-(20). In order to determine the worst-case realization of PV generation, the dispatched PV generation is

equal to the lower or upper bound as enforced by (21). Here $\sigma_{v,t}^{\varphi}$ is an auxiliary binary variable. The hourly real power dispatch of EV cluster $e(P_{e,t}^{\varphi})$ is formulated as (22) where $P_{e,t}^{\varphi,ch}$ and $P_{e,t}^{\varphi,dc}$ represent the charging and discharging powers of EV cluster e respectively. The charging and discharging powers for EV fleet e are limited by the charging and discharging power capacity $(P_e^{max,ch},P_e^{max,dc})$ as shown in (23) and (24) respectively. Here $IC_{e,t}$ is a binary parameter representing the connection of EV cluster e to the distribution network. If the EV cluster e is connected to the distribution network $IC_{e,t} = 1$ and otherwise, $IC_{e,t} = 0$. The relationship between the available energy in EV cluster e and the hourly power dispatch is shown in (25)-(26) using big-M method. The energy in the EV cluster is limited by the minimum and maximum values as shown in (27)-(28). The available energy in EV cluster is enforced at arrival and departure times by (29)-(32). Here, $I_{e,t}^{ar}$ and $I_{e,t}^{dep}$ are binary parameters that represent the arrival and departure at time t respectively. The slack variables are positive as shown in (33).

are positive as shown in (35).

$$\lim_{\substack{u_{v,t}^{\varphi}, l_{v,t}^{\varphi}, v_{v,t}^{\varphi} \\ v_{t}, v_{t}, v_{v,t}}} \sum_{\substack{v}} \sum_{\sigma} \sum_{t} \left[V_{v,t}^{\varphi} - (u_{v,t}^{\varphi} - l_{v,t}^{\varphi}) / P_{v}^{\varphi, max} \right] + \\
\max_{\sigma_{v,t}} \min_{\substack{s \\ s_{b,t}^{(), \varphi} \\ s_{b,t}^{(), \varphi}}} s_{b,t}^{1, \varphi} + s_{b,t}^{2, \varphi} + s_{b,t}^{3, \varphi} + s_{b,t}^{4, \varphi} \tag{1}$$

$$\begin{split} & \sum_{l} A L_{lb} \cdot P L_{l,t}^{\varphi} + \sum_{i} A I_{ib} \cdot P_{i,t}^{\varphi} + \sum_{v} A V_{vb} \cdot P_{v,t}^{\varphi} - \sum_{e} A E_{eb} \cdot \\ & P_{e,t}^{\varphi} + \sum_{n} A N_{nb} \cdot P_{n,t}^{\varphi} + s_{b,t}^{1,\varphi} - s_{b,t}^{2,\varphi} = \sum_{d} A D_{db} \cdot P_{d,t}^{\varphi} \\ & \sum_{l} A L_{lb} \cdot Q L_{l,t}^{\varphi} + \sum_{i} A I_{ib} \cdot Q_{i,t}^{\varphi} + \sum_{v} A V_{vb} \cdot Q_{v,t}^{\varphi} + \sum_{n} A N_{nb} \cdot \end{split}$$

$$Q_{n,t}^{\varphi} + s_{b,t}^{3,\varphi} - s_{b,t}^{4,\varphi} = \sum_{d} AD_{db} \cdot Q_{d,t}^{\varphi}$$
(3)

$$U_{k,t} - U_{b,t} + \widetilde{Z}_{l} \cdot \left(SL_{l,t}\right)^{*} + \widetilde{Z}_{l}^{*} \cdot SL_{l,t} \leq M \cdot p_{l}^{\varphi}$$

$$\tag{4}$$

$$-M \cdot p_{l}^{\varphi} \leq U_{k,t} - U_{h,t} + \widetilde{Z}_{l} \cdot (SL_{l,t})^{*} + \widetilde{Z}_{l}^{*} \cdot SL_{l,t}$$

$$(5)$$

$$-M \cdot p_l^{\varphi} \le U_{k,t} - U_{b,t} + \widetilde{Z}_l \cdot (SL_{l,t})^* + \widetilde{Z}_l^* \cdot SL_{l,t}$$

$$-p_l^{\varphi} \cdot SL_l^{\varphi,max} \le PL_{l,t}^{\varphi} \le p_l^{\varphi} \cdot SL_l^{\varphi,max}$$
(6)

$$-p_l^{\varphi} \cdot SL_l^{\varphi,max} \le QL_{l,t}^{\varphi} \le p_l^{\varphi} \cdot SL_l^{\varphi,max} \tag{7}$$

$$\begin{aligned} &-p_l^{\varphi} \cdot SL_l^{\varphi} &\leq PL_{l,t} \leq p_l^{\varphi} \cdot SL_l^{\varphi} & (0) \\ &-p_l^{\varphi} \cdot SL_l^{\varphi,max} \leq QL_{l,t}^{\varphi} \leq p_l^{\varphi} \cdot SL_l^{\varphi,max} & (7) \\ &-\sqrt{2} \cdot p_l^{\varphi} \cdot SL_l^{\varphi,max} \leq PL_{l,t}^{\varphi} + QL_{l,t}^{\varphi} \leq \sqrt{2} \cdot p_l^{\varphi} \cdot SL_l^{\varphi,max} & (8) \\ &-\sqrt{2} \cdot p_l^{\varphi} \cdot SL_l^{\varphi,max} \leq PL_{l,t}^{\varphi} - QL_{l,t}^{\varphi} \leq \sqrt{2} \cdot p_l^{\varphi} \cdot SL_l^{\varphi,max} & (9) \end{aligned}$$

$$-\sqrt{2} \cdot p_i^{\varphi} \cdot SL_i^{\varphi,max} \le PL_{i,t}^{\varphi} - QL_{i,t}^{\varphi} \le \sqrt{2} \cdot p_i^{\varphi} \cdot SL_i^{\varphi,max} \tag{9}$$

$$0 \le P_{i,t}^{\varphi} \le P_{i,\omega}^{max} \tag{10}$$

$$-Q_{i,\omega}^{max} \le Q_{i,t}^{\varphi} \le Q_{i,\omega}^{max} \tag{11}$$

$$P_{n,t}^{\varphi} \le \tan(\cos^{-1} PF_n) \cdot Q_{n,t}^{\varphi} \tag{12}$$

$$P_{n,t}^{\varphi} \ge -tan(\cos^{-1}PF_n) \cdot Q_{n,t}^{\varphi} \tag{13}$$

$$0 \leq P_{i,t}^{\varphi} \leq P_{i,\varphi}^{max}$$

$$-Q_{i,\varphi}^{max} \leq Q_{i,t}^{\varphi} \leq Q_{i,\varphi}^{max}$$

$$11)$$

$$P_{n,t}^{\varphi} \leq tan(\cos^{-1}PF_n) \cdot Q_{n,t}^{\varphi}$$

$$12)$$

$$P_{n,t}^{\varphi} \geq -tan(\cos^{-1}PF_n) \cdot Q_{n,t}^{\varphi}$$

$$13)$$

$$0 \leq P_{v,t}^{\varphi} \leq P_{v}^{\varphi,max}$$

$$-Q_{v}^{\varphi,max} \leq Q_{v,t}^{\varphi} \leq Q_{v}^{\varphi,max}$$

$$15)$$

$$-Q_v^{\varphi,max} \le Q_{v,t}^{\varphi} \le Q_v^{\varphi,max} \tag{15}$$

$$P_{v,t}^{\varphi} \le A_v^{\varphi} \cdot IR_{v,t} \tag{16}$$

$$P_{v,t}^{\varphi} \leq A_{v}^{\varphi} \cdot IR_{v,t}$$
 (16)
$$0 \leq l_{v,t}^{\varphi} \leq u_{v,t}^{\varphi}$$
 (17)
$$u_{v,t}^{\varphi} \leq P_{v}^{\varphi,max}$$
 (18)
$$(P_{v}^{\varphi,max} - A_{v}^{\varphi} \cdot IR_{v,t}) \cdot V_{v,t}^{\varphi} - l_{v,t}^{\varphi} \geq -A_{v}^{\varphi} \cdot IR_{v,t}$$
 (20)
$$A_{v}^{\varphi} \cdot IR_{v,t} \cdot V_{v,t}^{\varphi} + u_{v,t}^{\varphi} \leq A_{v}^{\varphi} \cdot IR_{v,t}$$
 (21)
$$P_{v,t}^{\varphi} = l_{v,t}^{\varphi} + (u_{v,t}^{\varphi} - l_{v,t}^{\varphi}) \cdot \sigma_{v,t}^{\varphi}$$
 (21)
$$P_{e,t}^{\varphi} = P_{e,t}^{\varphi,ch} - P_{e,t}^{\varphi,dc}$$
 (22)
$$0 \leq P_{e,t}^{\varphi,ch} \leq IC_{e,t}P_{e}^{max,ch}$$
 (23)
$$0 \leq P_{e,t}^{\varphi,dc} \leq IC_{e,t}P_{e}^{max,dc}$$
 (24)
$$E_{e,t}^{\varphi} - E_{e,t-1}^{\varphi} - P_{e,t}^{\varphi} \leq M \cdot (1 - IC_{e,t})$$
 (25)

$$u_{v,t}^{\varphi} \le P_v^{\varphi,max} \tag{18}$$

$$(P^{\varphi,max} - A^{\varphi} IR) V^{\varphi} - I^{\varphi} > -A^{\varphi} IR \tag{19}$$

$$\left(P_v^{\varphi, max} - A_v^{\varphi} . IR_{v,t} \right) . V_{v,t}^{\varphi} - l_{v,t}^{\varphi} \ge -A_v^{\varphi} . IR_{v,t}
 A_v^{\varphi} . IR_{v,t} . V_{v,t}^{\varphi} + u_{v,t}^{\varphi} \le A_v^{\varphi} . IR_{v,t}$$
(19)

$$P_{n,t}^{\varphi} = l_{n,t}^{\varphi} + (u_{n,t}^{\varphi} - l_{n,t}^{\varphi}) \cdot \sigma_{n,t}^{\varphi}$$
(21)

$$P_{e,t}^{\varphi} = P_{e,t}^{\varphi,ch} - P_{e,t}^{\varphi,dc} \tag{22}$$

$$0 \le P_{\varphi,ch}^{\varphi,ch} \le IC_{\varphi,t}P_{\varphi}^{max,ch} \tag{23}$$

$$0 \le P_{e,t}^{\varphi,dc} \le IC_{e,t}P_e^{max,dc} \tag{24}$$

$$E_{e,t}^{\varphi} - E_{e,t-1}^{\varphi} - P_{e,t}^{\varphi} \le M \cdot (1 - IC_{e,t})$$
 (25)

$$\begin{split} E_{e,t}^{\varphi} - E_{e,t-1}^{\varphi} - P_{e,t}^{\varphi} &\geq -M \cdot \left(1 - IC_{e,t} \right) \\ E_{e,t}^{\varphi} &\leq M \cdot \left(1 - IC_{e,t} \right) + E_{e}^{max} \end{split} \tag{26}$$

$$E_{e,t}^{\varphi} \le M \cdot (1 - IC_{e,t}) + E_e^{max} \tag{27}$$

$$E_{e,t}^{\varphi} \ge -M \cdot \left(1 - IC_{e,t}\right) + E_e^{min} \tag{28}$$

$$E_{et}^{\varphi} \le M \cdot \left(1 - I_{et}^{ar}\right) + E_e^{ar} \tag{29}$$

$$E_{e,t}^{\varphi} \ge -M \cdot \left(1 - I_{e,t}^{ar}\right) + E_e^{ar} \tag{30}$$

$$E_{e,t}^{\varphi} \leq M \cdot \left(1 - I_{e,t}^{dep}\right) + E_{e}^{dep}$$

$$E_{e,t}^{\varphi} \geq -M \cdot \left(1 - I_{e,t}^{dep}\right) + E_{e}^{dep}$$

$$(32)$$

$$E_{\varrho,t}^{\varphi} \ge -M \cdot \left(1 - I_{\varrho,t}^{dep}\right) + E_{\varrho}^{dep} \tag{32}$$

$$s_{b,t}^1, s_{b,t}^2, s_{b,t}^3, s_{b,t}^4 \ge 0 \tag{33}$$

$$\mathbf{z}_{l} = \mathbf{r}_{l} + j\mathbf{x}_{l} \tag{34}$$

$$\tilde{\mathbf{Z}}_l = \mathbf{A} \odot \mathbf{z}_l \tag{35}$$

$$\mathbf{A} = \begin{bmatrix} 1 & e^{-j2\pi/3} & e^{j2\pi/3} \\ e^{j2\pi/3} & 1 & e^{-j2\pi/3} \\ e^{-j2\pi/3} & e^{j2\pi/3} & 1 \end{bmatrix}$$
(36)

$$\mathbf{SL}_{l,t} = \begin{bmatrix} PL_{l,t}^{a} + jQL_{l,t}^{a}, PL_{l,t}^{b} + jQL_{l,t}^{b}, PL_{l,t}^{c} + jQL_{l,t}^{c} \end{bmatrix}$$
(37)

$$SL_{l,t} = \left[PL_{l,t}^{a} + jQL_{l,t}^{a}, PL_{l,t}^{b} + jQL_{l,t}^{b}, PL_{l,t}^{c} + jQL_{l,t}^{c} \right]$$
(37)

$$\boldsymbol{U}_{b,t} = \left[\left(V_{b,t}^{a} \right)^{2} \, \left(V_{b,t}^{b} \right)^{2} \, \left(V_{b,t}^{c} \right)^{2} \right]^{T} \tag{38}$$

B. Solution Methodology

The proposed two-stage optimization problem is solved using the C&CG approach [12]. The problem is decomposed into a master problem (39)-(44) with decision variable x and subproblem (45)-(48) with decision variables y, s and σ .

$$\min_{x} c^{T} x + \eta \tag{39}$$

s.t.

$$Ax \le d \tag{40}$$

$$\eta \ge b^T s^l \tag{41}$$

$$Dy^l \le g, \qquad \forall l \le k$$
 (42)

$$Cy^l + s^l = f, \qquad \forall l \le k \tag{43}$$

$$(E + M\sigma_l^*)x + Gy^l = h, \quad \forall l \le k$$
(44)

Here x represents the vector of first-stage decision variables i.e. $[l_{v,t}^{\varphi}, u_{v,t}^{\varphi}, V_{v,t}^{\varphi}]$.

$$\max_{\sigma \in [0,1]} \min_{y,s \ge 0} b^T s \tag{45}$$

s.t.

$$Dy \le g \tag{46}$$

$$Cy + s = f (47)$$

$$Gy = h - (E + M\sigma)x^* \tag{48}$$

Here y represents the second-stage recourse decision variables i.e. $P_{v,t}^{\varphi}$, $P_{e,t}^{\varphi}$, $P_{n,t}^{\varphi}$, $P_{i,t}^{\varphi}$, $Q_{v,t}^{\varphi}$, $Q_{n,t}^{\varphi}$, $Q_{i,t}^{\varphi}$, $PL_{l,t}^{\varphi}$ and $QL_{l,t}^{\varphi}$ as well as the voltage magnitude on the buses (U_{ht}) . The dual form of the sub-problem is shown as follows:

$$Q = \max_{T} g^{T} \mu_{1} + f^{T} \mu_{2} + [h - (E + M\sigma)x^{*}]\mu_{3}$$
 (49)

$$D\mu_1 + C\mu_2 + G\mu_3 \le 0 (50)$$

$$\mu_2 \le b \tag{51}$$

The μ_1 , μ_2 and μ_3 are dual variables for constraints (46), (47) and (48) respectively. The C&CG algorithm is described

Step 1: Set iteration index k = 0, $LB = -\infty$, $UB = \infty$ and convergence index $\varepsilon = 10^{-3}$.

Step 2: Solve the master problem and obtain the optimal solution, x_{k+1}^* and η_{k+1}^* and update the $LB = c^T x_{k+1}^* + \eta_{k+1}^*$

Step 3: Solve the sub-problem and update the UB = $min\{UB, c^T x_{k+1}^* + Q_{k+1}^*\}$

Step 4: Check the convergence if $UB - LB < \varepsilon$ terminate otherwise k = k + 1, add constraints (41)-(44) and go to step

III. NUMERICAL ANALYSIS

In this paper, a modified IEEE-13 bus system for which the peak demand is shown in Table I. Four PV units and four dispatchable distributed generation units (DGs) are installed in the system. Tables II and III show the characteristics of the DG and PV units respectively. The PV units and DG1-DG3 are three-phase generation units and DG4 is a single-phase distributed generation unit connected to phase C. 30 singlephase EVs are connected to the system. Table IV shows the characteristics of EVs. Fig. 1 shows the demand and total PV generation profiles in the operation horizon. The following cases are considered:

Case 1 – Deterministic maximum PV generation and demand without EV

Case 2 – Deterministic maximum PV generation and demand with EV

Case 3 – Uncertainty in maximum PV generation, demand, state of charge (SoC) of EVs at arrival and departure times, capacity and maximum real power dispatch of EVs

TABLE I

DEMAND CHARACTERISTICS							
Node	Phase a	Phase a	Phase b	Phase b	Phase c	Phase c	
	(kW)	(kVAr)	(kW)	(kVAr)	(kW)	(kVAr)	
1	0	0	0	0	0	0	
2	0	0	218.5	125.4	0	0	
3	0	0	161.5	118.75	0	0	
4	16.15	9.5	62.7	36.1	111.15	17.1	
 5	0	0	0	0	0	0	
6	152	104.5	114	85.5	114	85.5	
7	0	0	0	0	161.5	76	
8	0	0	0	0	0	0	
9	365.75	209	365.75	209	365.75	209	
10	0	0	0	0	161.5	143.45	
11	460.75	180.5	64.6	57	275.5	201.4	
12	121.6	81.7	0	0	0	0	
13	0	0	0	0	0	0	
Total	1116.25	585.2	987.05	631.75	1189.4	732.45	

TABLE II

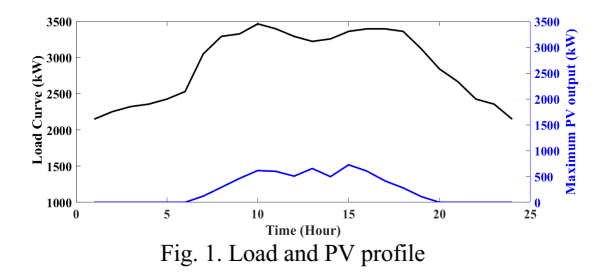
DISPATCHABLE DG UNITS' CHARACTERISTICS							
DG	Bus	P^{min}	P ^{max}	Q^{min}	Q^{max}		
1	4	0	200	-145	145		
2	6	0	200	-145	145		
3	13	0	250	-180	180		
4	7	0	40	-20	20		

TABLE III

PV GENERATION UNITS' CHARACTERISTICS							
PV	Bus	P^{min}	P^{max}	Q^{min}	Q^{max}		
1	13	0	200	-100	100		
2	10	0	200	-100	100		
3	9	0	200	-100	100		
4	4	0	100	-50	50		

TABLE IV CHARACTERISTICS OF EV UNITS

EV cluster	# of vehicles	Bus	P^{max}	E^{min}	E^{max}
1	15	4	45	0	450
2	15	10	45	0	450



1) Case 1 – Deterministic maximum PV generation and demand without EV

In this case, the maximum PV generation and demand are considered as forecasted values. The dispatchability limits of PV generation for each phase are shown in Fig. 3. The dispatchability limits for the PV generation units on phase A are shown in Fig. 3(a). In this case, the lower bound of dispatchability limit is increasing from 0 at hour 9 to 32.917 kW and 10.592 kW at hours 10 and 11 respectively. Here, the total real power demand at hour 10 is 1116.25 kW and the total dispatch of DG and main feeder, at hour 10, cannot increase beyond 1083.33 kW as the DGs reach their maximum capacity and feeder also reach the maximum apparent power capacity on this phase. Consequently, the lower dispatchability limit for the PV generation at hour 10 on phase A reaches 32.917 kW.

2) Case 2 – Deterministic maximum PV generation and demand with EV.

In this case, the dispatchability limits for PV generation units are evaluated considering the EVs and forecasted maximum PV generation and demand. Five EVs are connected to each phase on buses 4 and 10. All EVs in each cluster, are considered as the same type. The maximum charging and discharging power for each EV is 3kW and maximum energy capacity is 30kWh. The arrival and departure times for EVs are 10:00 and 19:00 respectively. It is assumed that the EVs remain connected to the network within the arrival and departure times and EVs have bi-directional power capability (V2G enabled). The EVs are assumed to have 20% SoC at arrival time. The state of charge (in percent) is defined as the ratio between the available energy in EV clusters and the maximum capacity of the EV clusters. Fig. 3 shows the upper and lower bounds for dispatchability limits of PV generation when the SoC of EV clusters at the departure time is 100%. In this case, the lower bound for dispatchability limit on phase C, at hour 10 is reduced by 30 kW compared to that in Case 1 and reached 116.383 kW. At hour 10, 30 kW is injected by the EV clusters to reduce the lower bound for PV dispatchability limit. At hour 11, the lower bound for dispatchability limit in Case 1 was 107.946 kW and it increases to 137.946kW in this case as the batteries of EV clusters on phase C are being charged by 30kW. Fig. 3 also shows the impact of vehicle-to-grid (V2G). When EV clusters are unable to inject power back to the grid (no V2G), the lower bound for PV generation is higher or equal to the lower bound in Case 1.

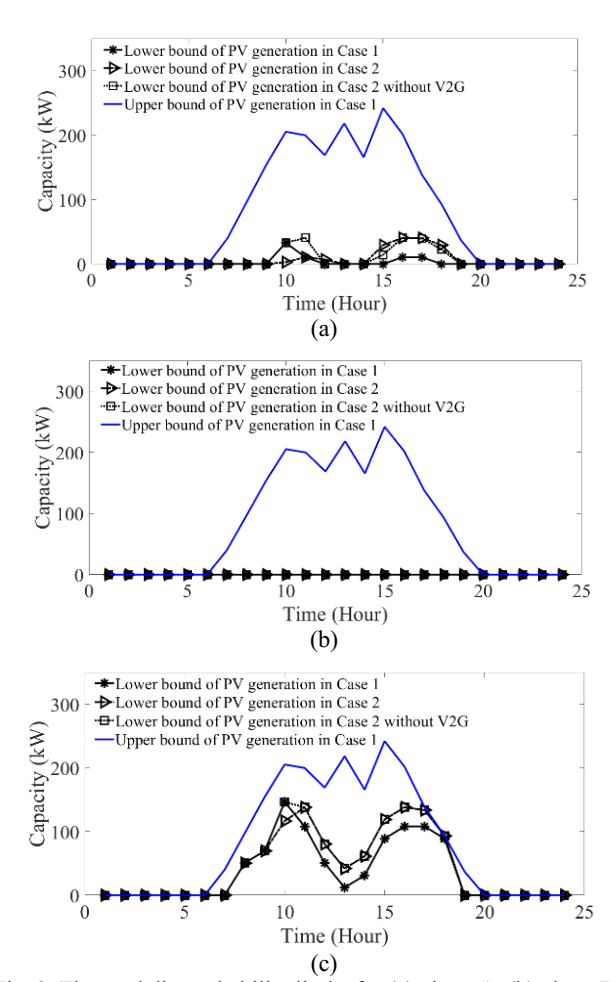


Fig. 3. The total dispatchability limits for (a) phase A, (b) phase B and (c) phase C with deterministic demand and maximum PV generation with and without EV clusters

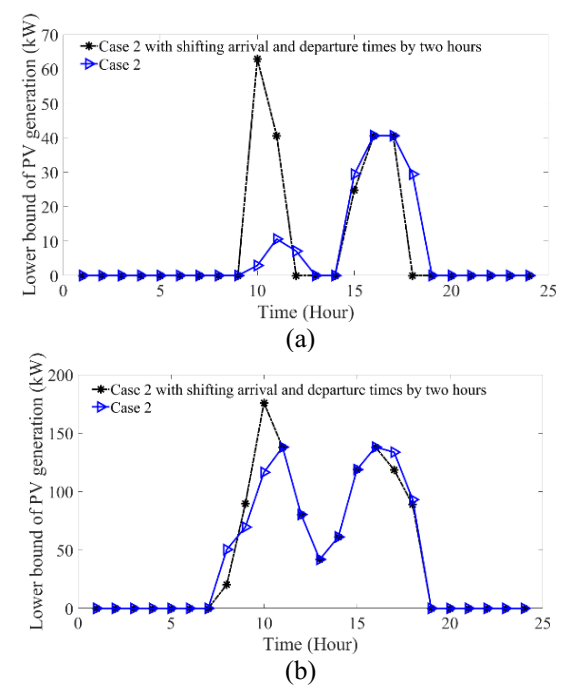


Fig. 4. The effects of arrival and departure time on the total dispatchability limits for (a) phase A, (b) phase C

Fig. 4 shows the lower bound for the dispatchability limit of PV generation on phase A and phase C for Case 2 with two hours shifting in arrival and departure times. The SoC of EVs at the departure time is 100 percent. As shown in Fig 4(a), on phase A, the lower bound at hours 10 and 11, are increased from 2.917 kW and 10.592kW to 62.917 kW and 40.592 kW when the arrival and departure times are shifted by two hours. In phase C as it is shown in Fig. 4(b), the lower bound at hour 8 is decreased from 50.291kW to 20.291kW when the arrival and departure times are shifted by two hours.

3) Case 3 – Uncertainty in maximum PV generation, demand, state of charge (SoC) of EVs at arrival and departure times, capacity and maximum real power dispatch of EVs

In this case, the forecast error for maximum PV generation, load, SoC of EVs at arrival and departure times, capacity and maximum real power dispatch of EV clusters are represented by a normal distribution function with a mean equal to those in Case 2. The standard deviation for maximum PV generation and demand is 0.0167 of the mean value and the standard deviation for the SoC of EV clusters at the departure and arrival times, capacity and maximum real power dispatch of EV clusters are 0.06 of the mean values. In this case, 200 scenarios are considered. The expected upper bound and lower bounds for dispatchability limits of PV generation units and those for Case 2 are shown for phases A and C in Fig. 5(a) and Fig. 5(b) respectively.

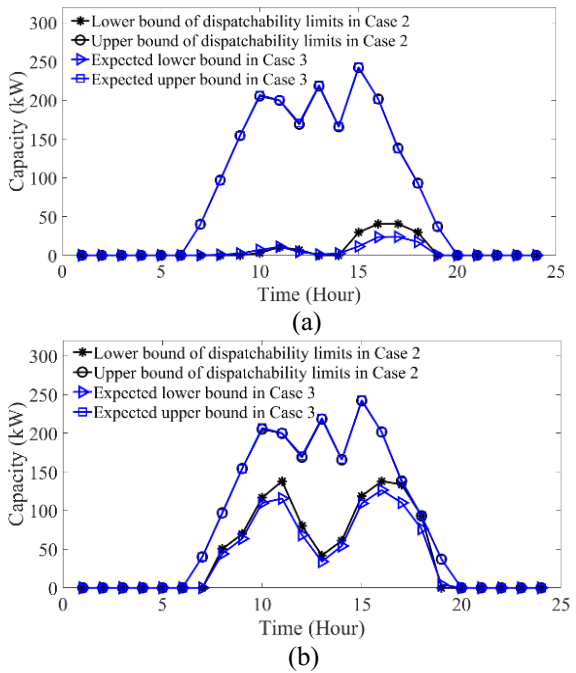


Fig. 5. The expected dispatchability limits of PV generation considering the uncertainty in maximum PV generation, SoC of EV clusters at the arrival and departure times and demand, (a) phase A (b) phase C

IV. CONCLUSION

In this paper, the dispatchability limit for PV generation in the unbalanced distribution networks is quantified. It is shown that EV clusters with no V2G will increase the lower bound of dispatchability of PV generation. While V2G can reduce the lower bound for dispatchability limits of PV generation, integrating EVs into the distribution network will increase the lower bound for the dispatchability limit of PV generation as the EVs are being charged for departure. Furthermore, the impact of arrival and departure times for EV clusters are shown in the case study.

REFERENCES

- [1] K. Clement-Nyns, E. Haesen and J. Driesen, "The Impact of Charging Plug-In Hybrid Electric Vehicles on a Residential Distribution Grid," *IEEE Transactions on Power Systems*, vol. 25, no. 1, pp. 371-380, Feb. 2010.
- [2] G. Razeghi, et al. "Impacts of plug-in hybrid electric vehicles on a residential transformer using stochastic and empirical analysis," *Journal of power sources* vol. 252, pp. 277-285, Apr. 2014. [3] A. S. Masoum, S. Deilami, A. Abu-Siada, and M. A. S. Masoum, "Fuzzy Approach for Online Coordination of Plug-In Electric Vehicle Charging in Smart Grid," *IEEE Transactions on Sustainable Energy*, vol. 6, no. 3, pp. 1112-1121, July 2015.
- [4] Seguin, Rich, et al. *High-penetration PV integration handbook for distribution engineers*. No. NREL/TP-5D00-63114. National Renewable Energy Lab. (NREL), Golden, CO U.S., 2016.
- [5] M. Shafie-Khah, P. Siano, D. Z. Fitiwi, N. Mahmoudi, and J. P. S. Catalão, "An Innovative Two-Level Model for Electric Vehicle Parking Lots in Distribution Systems with Renewable Energy," *IEEE Transactions on Smart Grid*, vol. 9, no. 2, pp. 1506-1520, March 2018.
- [6] T. Ding, C. Li, Y. Yang, J. Jiang, Z. Bie and F. Blaabjerg, "A Two-Stage Robust Optimization for Centralized-Optimal Dispatch of Photovoltaic Inverters in Active Distribution Networks," *IEEE Transactions on Sustainable Energy*, vol. 8, no. 2, pp. 744-754, April 2017.
- [7] H. Ji, C. Wang, P. Li, F. Ding, and J. Wu, "Robust Operation of Soft Open Points in Active Distribution Networks with High Penetration of Photovoltaic Integration," *IEEE Transactions on Sustainable Energy*, vol. 10, no. 1, pp. 280-289, Jan. 2019.
- [8] J. Zhao, T. Zheng, and E. Litvinov, "Variable Resource Dispatch Through Do-Not-Exceed Limit," *IEEE Transactions on Power Systems*, vol. 30, no. 2, pp. 820-828, March 2015.
- [9] Z. Li, F. Qiu, and J. Wang. "Data-driven real-time power dispatch for maximizing variable renewable generation." *Applied Energy*, vol. 170, pp. 304-313, May 2016.
- [10] B. Chen, C. Chen, J. Wang, and K. L. Butler-Purry, "Sequential Service Restoration for Unbalanced Distribution Systems and Microgrids," *IEEE Transactions on Power Systems*, vol. 33, no. 2, pp. 1507-1520, March 2018.
- [11] X. Chen, W. Wu, and B. Zhang, "Robust Restoration Method for Active Distribution Networks," *IEEE Transactions on Power Systems*, vol. 31, no. 5, pp. 4005-4015, Sept. 2016.
- [12] B. Zeng, Bo, and L. Zhao. "Solving two-stage robust optimization problems using a column-and-constraint generation method," *Operations Research Letters* vol. 41, no .5, pp. 457-461, Sept. 2013.